Journal of NeuroVirology, 8: 204–210, 2002
 ISSN 1355–0284/02 $12.00+.00
DOI: 10.1080/13550280290049642

The relationship of herpes simplex virus latency associated transcript expression to genome copy number: A quantitative study using laser capture microdissection

Xiao-Ping Chen,[1] Marina Mata,[1,3] Mary Kelley,[3] Joseph C Glorioso,[2] and David J Fink,[1,2,3]

[1]*Departments of Neurology and* [2]*Molecular Genetics and Biochemistry, University of Pittsburgh School of Medicine, Pittsburgh, Pennsylvania; and* [3]*GRECC, VA Medical Center, Pittsburgh, Pennsylvania, USA*

To investigate the quantitative relationship of latent herpes simplex virus (HSV) genomes to the expression of latency associated transcripts (LATs) we used a combination of laser capture microdissection (LCM), polymerase chain reaction (PCR), and quantitative real-time PCR to determine the number of HSV genomes in individual neurons of the mouse trigeminal ganglion (TG) during viral latency. Both LAT-positive and LAT-negative neurons detected by *in situ* hybridization (ISH) and lifted by LCM contained HSV genomes detected by PCR for HSV ICP47. The number of genomes/cell determined by real-time PCR with probes for HSV UL44 following LCM demonstrated a Poisson distribution with a predicted mean count of 178 genomes/LAT-positive neuron, and 68 genomes/LAT-negative neuron. The range was similar between the LAT-positive and LAT-negative neurons, and there was a substantial overlap in the distributions. These results suggest that the expression of LATs in an amount that is detectable by ISH does not depend only on the number of HSV genomes in the cell, and by implication suggests that neuron-specific factors play a role in the regulation of LAT expression during latency. *Journal of NeuroVirology* (2002) **8,** 204–210.

Keywords: herpes simplex virus; latency; latency associated transcript (LAT); real-time PCR; laser capture microdissection

Introduction

Herpes simplex virus (HSV) characteristically establishes a lifelong latent state in neurons. The existence of latent genomes in sensory ganglia was first inferred from the ability of virus to be reactivated from infected ganglia that no longer harbor infectious virus, and subsequently confirmed on the cellular level by the detection of latency associated transcripts (LATs), abundant nonpolyadenylated RNA transcripts found in the nucleus of neurons of latently infected individuals (Rock *et al*, 1987; Stevens *et al*, 1987; Krause *et al*, 1988; Steiner *et al*, 1988; Stevens *et al*, 1988). There have been conflicting reports regarding the role of LAT expression in the establishment of the latent state, or reactivation of virus from latency (Leib *et al*, 1989; Bergstrom and Lycke, 1990; Hill *et al*, 1990; Trousdale *et al*, 1991; Thompson and Sawtell, 1997). The ability to quantify viral burden at the level of single cells is essential for understanding many aspects of latency and reactivation (Sawtell, 1997).

The estimated total number of latent genomes per ganglion reported in the literature varies widely, in part depending on the method used to calculate that number, with estimates ranging from 3500 genomes per ganglion determined by semiquantitative Southern blot (Sedarati *et al*, 1989) or semiquantitative PCR

Address correspondence to Dr David Fink, S-520 BST, 200 Lothrop Street, Pittsburgh, PA 15213, USA. E-mail: dfink@pitt.edu

This work was supported by grants from the NIH (JCG and DJF) and the Department of Veteran's Affairs (MM and DJF). We acknowledge the excellent technical assistance of Ms. XiaoPing Hu, Mindi Zhang, and Veljko Puskovic.

Received 20 January 2002; revised 25 February 2002; accepted 4 March 2002.

(Rodahl and Stevens, 1992) to 10^5 genomes determined by other PCR-based methods (Katz *et al*, 1990; Ramakrishnan *et al*, 1994). Combining *in situ* hybridization with PCR techniques, and making the assumption that only cells that are LAT-positive by ISH contain HSV genomes, Hill calculated the presence of 17 to 34 genomes per LAT-positive cell (Hill *et al*, 1996) in latently infected rabbit trigeminal ganglion (TG). In a more comprehensive analysis, using semiquantitative PCR to determine the number of genomes in neurons dissociated from latently infected fixed TG, Sawtell determined that 20% of the neurons in a TG infected by $17syn^+$ strain of HSV contained HSV genomes, and that the number of latent genomes ranged from less than 10 to more than 1000 per neuron (Sawtell, 1997). TG infected with KOS strain HSV contained substantially fewer latent genomes per cell than TG infected by *Syn*17 (Sawtell *et al*, 1998).

LATs are detected by ISH in only 0.1% to 3% of the neurons in latently infected ganglia (Roizman and Sears, 1996), but more sensitive *in situ* PCR techniques demonstrate that latent genomes are present in neurons that are LAT-positive by ISH, as well as LAT-negative by ISH (Ramakrishnan *et al*, 1994, 1996; Mehta *et al*, 1995). The relationship between the number of latent genomes in an individual neuron to the expression of LATs detectable by ISH has not previously been investigated. One possibility is that expression of LATs to a level detectable by ISH is a function of the number of latent HSV genomes in the cell. According to this hypothesis, LATs would be detected when the number of latent genomes exceeded a threshold value. The alternative possibility is that LAT expression from latent HSV genomes depends on the presence of cell-specific factors within the host cell. According to this alternate hypothesis, the number of latent HSV genomes in LAT-positive and LAT-negative cells would display a similar distribution. To test the two hypotheses, we combined the methods of laser capture microdissection (LCM) and quantitative real time PCR with ISH to determine the number of genomes per neuron in latently infected ganglia, in order to establish the distribution of latent genomes in TG at the single cell level, and to examine the relationship of the number of latent genomes to the expression of LATs detectable by ISH.

Results

We first determined the number of LAT-positive cells during latency using ISH. At 30 days after corneal scarification with HSV KOS, the number of neurons in the DRG demonstrating the presence of LAT by ISH was determined by counting all of the LAT-positive cells in every fifth cryostat section. There were 14–28 positive cells per section, and approximately 200 LAT-positive cells in each ganglion. This number, which is equivalent to 1% of the neurons in the ganglion (assuming that there are approximately 20,000 neurons in a mouse TG), is well within the range of previous reports of the number of LAT-positive cells determined by ISH (Roizman and Sears, 1996).

In order to determine whether HSV genomes could be detected in LAT-negative cells, groups of 10

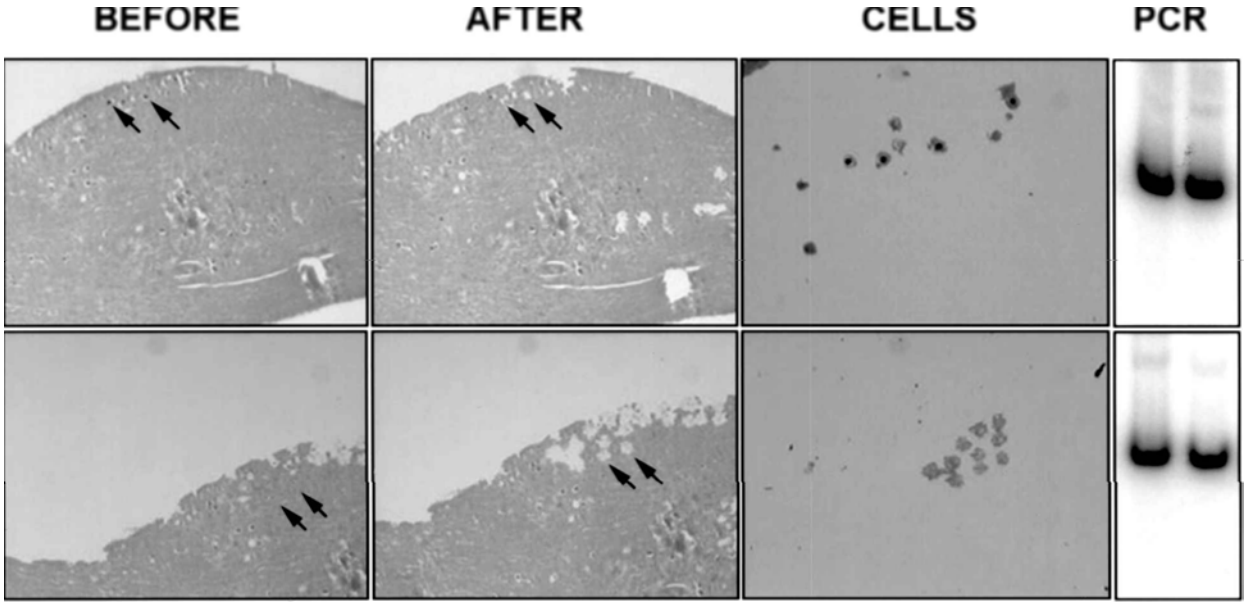

Figure 1 HSV DNA from LAT-positive and LAT-negative neurons of TG lifted by LCM. 30 days after infection by corneal scarification LAT expression was detected by ISH. 10 LAT-positive neurons (upper panel, arrows point to examples of LAT-positive cells) and 10 LAT-negative neurons (lower panels, arrows point to examples) were collected by LCM, and the presence of HSV DNA determined by PCR for HSV ICP47 (right column). The same TG section before LCM, after LCM, and the cells lifted onto the cap are shown as labeled. Two PCR reactions from separate groups of 10 neurons for each condition are presented.

LAT-positive neurons from the sectioned ganglion were microdissected onto a single cap (Figure 1, top row) and 10 LAT-negative neurons from the same slide (Figure 1, bottom row) captured onto the thermoplastic film-coated PCR tube cap in an identical fashion using a 15-μM laser beam. The presence of HSV genomes in the microdissected cells was assessed by PCR using primers for HSV ICP47. Both the LAT-positive and the LAT-negative cells were positive for HSV genomes by PCR (Figure 1, right column). Uninfected control ganglia were negative for HSV by PCR (data not shown). This result is in agreement with previous observations, obtained using *in situ* PCR, demonstrating that both LAT-positive and LAT-negative cells in latently infected TG contain HSV genomes (Mehta *et al*, 1995; Ramakrishnan *et al*, 1994, 1996), but is not informative regarding the quantitative aspects of latency in LAT-positive and LAT-negative cells.

In order to determine how many HSV genomes were present in the LAT-positive and LAT-negative cells we repeated the experiment, infecting five mice by corneal scarification with HSV-1 KOS using the same protocol. At 30 days postinoculation the animals were sacrificed and one trigeminal ganglion from each animal was homogenized for determination of the total number of HSV genomes by real-time PCR with primers and probes for HSV UL44. The total number of HSV genomes in the whole ganglia lysate ranged from 1.7×10^4 to 9.8×10^5 with mean value of 7.3×10^4 genomes per ganglion. This number is similar to that previously reported by our group using quantitative PCR (Ramakrishnan *et al*, 1994) and the number obtained by others employing other PCR-based techniques (Sawtell, 1998).

The second ganglion from each pair was cryostat sectioned, processed for the presence of LATs by ISH using the digoxigenin-labeled probe, and individual LAT-positive and LAT-negative neurons then microdissected by LCM (Figure 2). The number of HSV genomes in the individually microdissected cells was established using real-time PCR. In agreement with the qualitative data, HSV genomes were found in both LAT-positive and LAT-negative cells. The number of HSV-1 genomes present in both LAT-positive and LAT-negative cells displayed a Poisson distribution (Figure 3) with a substantial overlap in the number of HSV genomes per cell between the LAT-positive and LAT-negative cells (Figure 3 and Table 1). Neurons microdissected from control TG by LCM contained essentially no detectable genomes, although an occasional false positive for a low number of genomes was seen (Figure 3 and Table 1). To compare the mean counts of genomes across groups (LAT-positive, LAT-negative, and control), we performed a Poisson regression with appropriate indicator variables for group. Because there was significant evidence of overdispersion in the Poisson model (test of $\alpha = 0$: $P < 0.0005$), we substituted a negative binomial model to reduce the effect of overdispersion on the significance tests. The predicted mean counts were 178 genomes/cell for the LAT-positive group, 68 genomes/cell for the LAT-negative group, and 4 for the control group. A specific test of the difference between the LAT-positive and LAT-negative groups, based on model estimates, was significant (Wald $\chi^2 = 4.37$, df $= 1$, $P = 0.0366$).

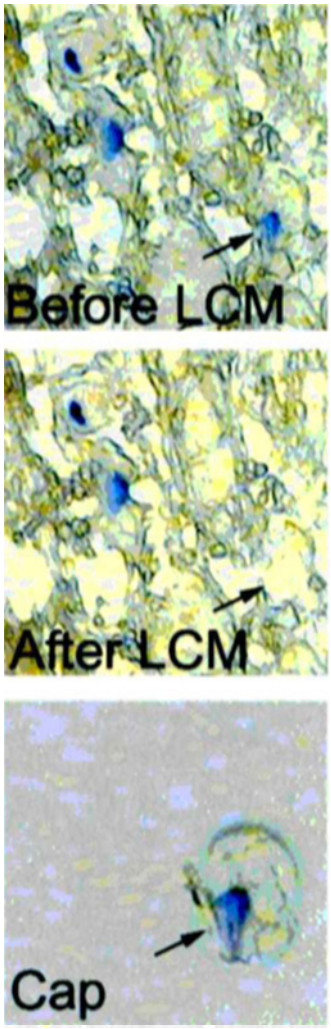

Figure 2 LCM of individual neurons for real-time PCR. A single LAT-positive neuron is shown before LCM (arrow, top) and the same section after LCM (arrow, middle). The lifted cell on the cap is shown at the bottom (arrow, higher magnification). The ISH signal for LAT appears blue in this micrograph of ISH performed with a digoxigenin-labeled probe, and two additional LAT-positive neurons are seen.

Discussion

The distribution of latent HSV genomes at a single cell level is an important parameter for understanding the establishment and reactivation of HSV from latency. The results of this study confirm and extend previous observations (Sawtell, 1997) made using semiquantitative PCR in conjunction with dissociation of fixed ganglia containing latent genomes

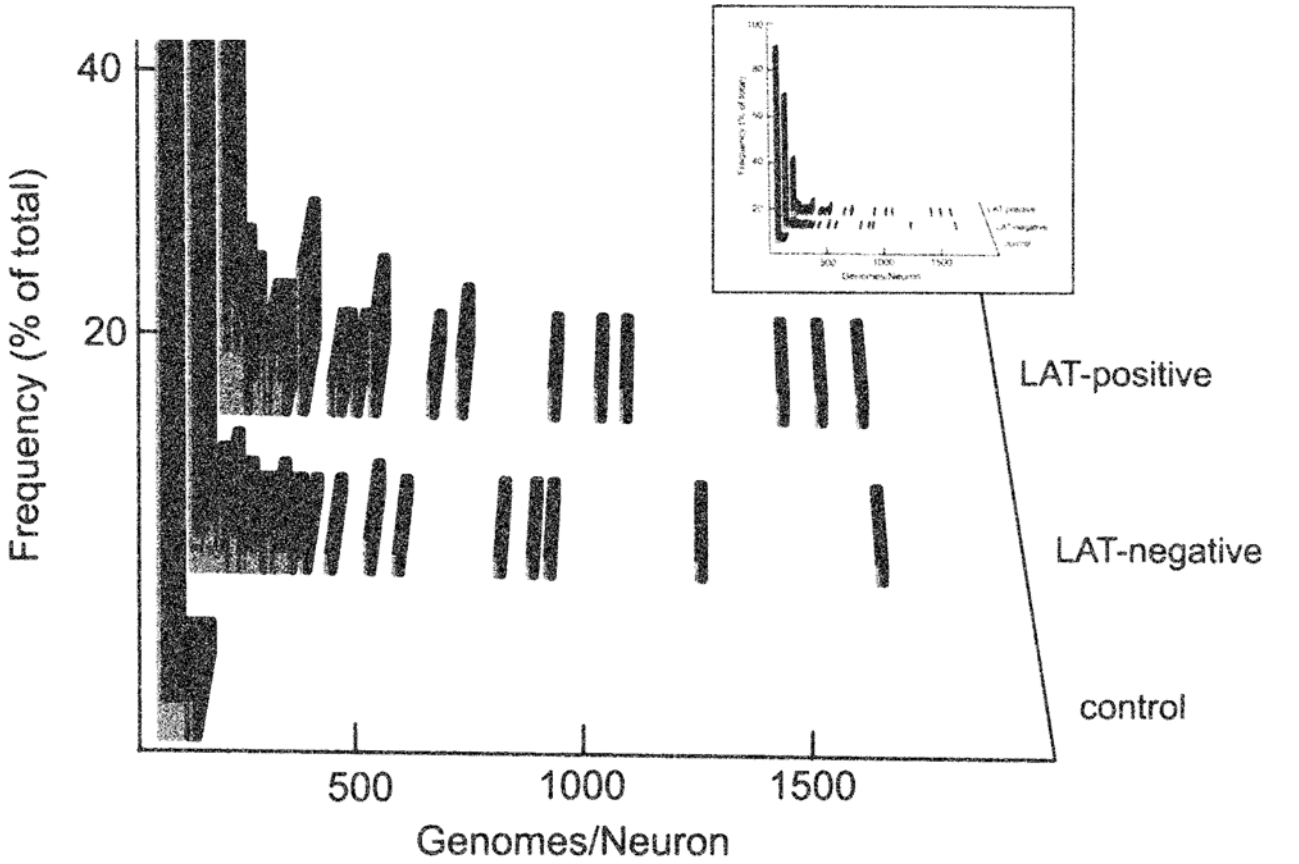

Figure 3 Quantitation of HSV genomes in individual neurons. The number of genomes per cell, determined by real-time PCR of individual neurons lifted by LCM is plotted for LAT-positive and LAT-negative cells in the ganglion, and control cells lifted from an uninfected ganglion. Cells were collected from 20 ganglion sections obtained from two different animals. The full range of number of genomes per cell was seen in cells from each animal, but the number of animals studied does not allow a formal statistical analysis of the variation between animals. The y axis is cut off at 40%. Inset shows the entire graph, including the full frequency of negative samples in the control and LAT-negative groups.

(contextual analysis) to analyze viral burden at the single cell level. According to that analysis the majority of latently infected TG neurons contain fewer than 10 genomes, with a smaller number containing 10–100 genomes, and fewer neurons containing up to 1000 genomes per cell (Sawtell, 1997). The overall distribution of genomes/neuron determined directly in our study by real time PCR combined with LCM is similar to that found by contextual analysis; the difference in absolute numbers may be a consequence of the difference in viral strain or the method employed.

Table 1 The number of HSV genomes/neuron determined by quantitative real-time PCR for individually microdissected LAT-positive (top row), LAT-negative (middle row), and control (bottom row) cells from TG 30 days after inoculation by corneal scarification. The number of cells in each group and the percentage of the total represented by that count is presented in the table

	HSV genomes/neuron							
ISH pattern	*0*		*10–300*		*300–1000*		*>1000*	
LAT-positive	30	38%	37	46%	9	11%	4	5%
LAT-negative	104	65%	47	29%	7	4%	2	1%
Control	37	93%	3	8%	0	0%	0	0%

In the current study we also confirmed using a different method, previous observations made using *in situ* PCR in conjunction with ISH (Ramakrishnan *et al*, 1994; Mehta *et al*, 1995), suggesting that LAT-negative cells also contain latent HSV genomes. The direct confirmation of this finding in cells microdissected from the same section used for ISH detection by a PCR method that is independent of histology serves as an important independent confirmation of the presence of HSV genomes in LAT-negative cells. It is possible that the presence of HSV genomes in cells that do not demonstrate LATs by ISH may reflect the limit of sensitivity of the *in situ* hybridization method. We are unable to retrieve RNA for RT-PCR analysis after the tissue has undergone the ISH procedure, so that we are unable to quantitate the amount or LAT RNA in the individual neurons. Nonetheless, the result demonstrates that the number of LAT-positive cells fails to represent the full distribution of neurons that contain genomes.

The novel finding of the current study is the observation that the number of genomes/neuron in the LAT-positive and LAT-negative groups overlap substantially (Figure 3). The predicted mean number of

genomes/neuron is higher in LAT-positive than in LAT-negative cells, a statistical difference that reflects the fact that there are a larger number of neurons containing detectable genomes in the LAT-positive group. But at any level of genomes/cell (ranging from 10 to more than 1500), both LAT-positive and LAT-negative cells are represented. This observation clearly demonstrates that there is no direct relationship between the number of genomes in the neuron during latency and the expression of LATs at a level that can be detected by ISH.

Although 38% of the LAT-positive cells in our study had no detectable genomes as assessed by quantitative real-time PCR, the fact that these cells expressed LATs were detectable by ISH indicates that these cells must actually contain HSV genomes. There are several possible explanations for this apparent discrepancy. The most likely explanation is that each of these cells contain fewer than 10 genomes per cell, and therefore falls below the limit of detection of the PCR method employed. We cannot exclude the possibility that some DNA was lost during tissue processing and microdissection, that the cell lifting was incomplete, or that the tissue section did not include the region of the nucleus containing latent genomes. And, 65% of the LAT-negative cells contained no HSV-genomes detected by real-time PCR. Although it is possible that LAT-negative cells with no detectable genomes by real-time PCR in fact contain no genomes, we think it is more likely that the same considerations described previously for the LAT-positive population of neurons apply, and that many of those cells also contain less than 10 (but more than 0) genomes per cell.

Further, 7.5–30% of neurons in the ganglion, depending on the titer applied to the cornea, are positive for HSV genomes determined using contextual analysis (Sawtell, 1997). Although the results of the current study are in general in agreement with that previous study, we found that at a minimum 62% of the LAT-positive cells and 35% of the LAT-negative cells contained detectable HSV genomes. There are several possible explanations for the difference between the previous results and the present study: (1) the difference in virus strain may be important; (2) the limit of sensitivity of contextual analysis for detecting fewer that 10 genomes/cell has not been determined; (3) and it is possible both that some genomes may be lost from cells during the dissociation process required for contextual analysis.

What determines whether a cell containing latent HSV genomes will express LATs at a level sufficient to detect by ISH? One possibility is that expression of LATs is a direct result of the number of genomes in the cell; past a threshold, detectable LATs are produced. Although there is a statistically significant difference between LAT-positive and LAT-negative cells in the distribution of genomes/cell, there is a substantial overlap in those distributions. These data suggest that the expression of LATs in an amount that is detectable by ISH is not simply a reflection of the number of HSV genomes in the cell, because cells with similar number of genomes may be LAT-positive or LAT-negative. The alternative possibility, supported by current study, is that some as yet undefined host cell factors are likely to be responsible for this difference in LAT expression between neurons harboring similar numbers of genomes. Further studies will be required to identify those host cell factors. The current study demonstrates that the combination of LCM and quantitative real-time PCR allows the analysis of HSV latency at a single cell level with a degree of precision that has not previously been possible.

Materials and methods

Virus and animals These studies were carried out with wild-type KOS strain HSV-1. Then, 4–8 weeks old female Balb/c mice were inoculated in both eyes with 5×10^6 p.f.u. in 5 μl by corneal scarification, and sacrificed under anesthesia 30–40 days after infection. The protocol for the animal studies was reviewed and approved by the institutional animal welfare committee.

***In situ* hybridization (ISH)** ISH for LATs was carried out as previously described (Ramakrishnan *et al*, 1994). Briefly, 10-μm cryostat sections of infected and control trigeminal ganglia were fixed with 4% paraformaldehyde for 30 min. After equilibration with 5× SSC for 10 min, the tissue was hybridized with a digoxigenin-labeled riboprobe antisense to the LAT sequence derived from a plasmid containing the bamHI B fragment of HSV (Gordon *et al*, 1988) at 56°C overnight. After washing with decreasing concentrations of buffer solution (from 2× SSC to 0.5× SSC), the bound digoxigenin-labeled probe was localized with an alkaline phosphatase-conjugated antidigoxigenin antibody (1:5000; Boehringer-Mannheim) detected with 5-bromo-4-chloro-3-indolylphosphate toluidium-nitroblue tetrazolium (BCIP-NBT; Vector Laboratories).

Laser capture microdissection (LCM) and polymerase chain reaction (PCR) Individual LAT-positive and LAT-negative neurons were microdissected from the slide after ISH by LCM using a PixCell LCM system (Arcturus Engineering, Santa Clara, CA). The sections were first dehydrated with two changes of 95% ethanol (2 min), two changes of 100% ethanol (2 min), and two changes of xylene (2 min) before being air dried. Cells were lifted onto a PCR cap (Arcturus Engineering) using a 15-μm laser beam, and groups of 10 cells on each cap analyzed for the presence of HSV genomes by PCR using primers specific for HSV ICP47 (forward primer 5′ GCG GTC GGA CGG CTT CAG ATG 3′; reverse primer 5′ CGG GCG ACC CAG ATG TTT ACT 3′) as described next.

The cells on the cap were dissolved in 20 μl lysis buffer containing 1× PCR buffer (Perkin-Elmer,

without $MgCl_2$), 1% Tween-20, and 0.4 mg/ml proteinase K at 37°C overnight. Proteinase K was heat inactivated at 99°C for 10 min. Then, 10 μl of cell lysate was used in a PCR reaction containing 1× PCR buffer, 2 mM $MgCl_2$, 200 μM each of dATP, dCTP, dGTP, and dTTP, 0.2 μM primers, 2.5 U HotStarTaq DNA Polymerase (Strategene), and 10 μCi ^{32}P-dCTP. The PCR reaction (performed in a Perkin-Elmer 480 thermal cycler) consisted of 15-min preincubation at 95°C, followed by 40 cycles of denaturing (94°C, 1 min), annealing (60°C, 1 min), and extension (72°C, 1 min), followed by a final extension of 10 min at 72°C. The PCR product was separated on a 5% acrylamide gel and detected by autoradiographic exposure for 16 h.

Real-time PCR analysis (fluorescent-based simultaneous amplification and product detection) The number of genomes in whole ganglia or individual cells microdissected by LCM from sectioned ganglia was quantitated by real-time PCR using primers and probes for the HSV UL44 (glycoprotein C) gene (Cohrs *et al*, 2000). Single cells lifted onto PCR caps were lysed as described above, and 10 μl of lysate added to 40 μl containing 900 nM of primers (forward primer 5′ GAT GCC GGT TTT GGA ATT C 3′; reverse primer 5′ CCC ATG GAG TAA CGC CAT ATC T 3′), 250 nM of probe (labeled at the 5′ end with the fluorescent reporter dye FAM and at the 3′ end with quencher dye TAMRA (Sythegen, Houston, TX), 5′ (FAM) ACC CGC ATG GAG TTC CGC CTC (TAMRA) 3′), and 1× TaqMan universal mix (Perkin-Elmer, Foster City, CA). After 2-min incubation at 50°C and 10 min of incubation at 95°C for denaturation, the samples were subjected to 50 cycles of PCR (95°C for 15 s and 60°C for 1 min) in a GenAmp 5700 Sequence Detector (Perkin-Elmer). Each PCR run contained two blank controls, serially diluted highly purified HSV DNA as standard, and the experimental samples run in duplicate. The number of genomes in each sample was determined by comparing the threshold cycle (Ct) value, defined as the amplification cycle at which a statistically significant increase is detected in the difference between the emission intensity of the reporter dye in the sample and the emission intensity of the controls without DNA, to a standard curve obtained using HSV-1 DNA.

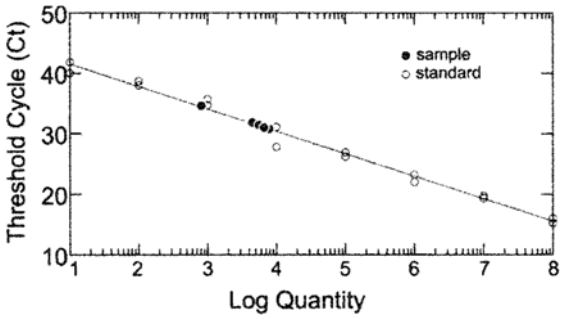

Figure 4 Real-time PCR quantitation of HSV genomes. Purified HSV-1 DNA was amplified by PCR of UL44; the threshold cycle (Ct) is plotted against the amount of input DNA.

To establish the standard curve, HSV-1 (KOS) DNA was purified with three rounds of phenol-chloroform extraction and ethanol precipitation. The viral DNA concentration was determined by UV spectrophotometer, and the DNA then serially diluted in nuclease-free water such that 1 μl of the sample contained 10^7, 10^6, 10^5, 10^4, 10^3, 10^2, or 10 copies of HSV-1 DNA. Next, 100 ng of mouse genomic DNA (Clontech, Palo Alto, CA) was added into each standard sample to mimic the DNA complexity of the virus-containing tissue samples. Real-time PCR amplification of HSV-1 DNA was linear over a range from 10 to 10^8 copies of HSV DNA (Figure 4).

References

Bergstrom T, Lycke E (1990). Neuroinvasion by herpes simplex virus. An *in vitro* model for characterization of neurovirulent strains. *J Gen Virol* **71**(Pt 2): 405–410.

Cohrs RJ, Randall J, Smith J, Gilden DH, Dabrowski C, van Der Keyl H, Tal-Singer R (2000). Analysis of individual human trigeminal ganglia for latent herpes simplex virus type 1 and varicella-zoster virus nucleic acids using real-time PCR. *J Virol* **74**(24): 11464–11471.

Gordon YJ, Johnson B, Romanowski E, Araullo-Cruz T (1988). RNA complementary to herpes simplex virus type I ICP0 gene demonstrated in neurons of human trigeminal ganglia. *J Virol* **62:** 1832–1835.

Hill JM, Gebhardt BM, Wen R, Bouterie AM, Thompson HW, O'Callaghan RJ, Halford WP, Kaufman HE (1996). Quantitation of herpes simplex virus type 1 DNA and latency-associated transcripts in rabbit trigeminal ganglia demonstrates a stable reservoir of viral nucleic acids during latency. *J Virol* **70**(5): 3137–3141.

Hill JM, Sedarati F, Javier RT, Wagner EK, Stevens JG (1990). Herpes simplex virus latent phase transcription facilitates *in vivo* reactivation. *Virology* **174:** 117–125.

Katz JP, Bodin ET, Coen DM (1990). Quantitative polymerase chain reaction analysis of herpes simplex virus DNA in ganglia of mice infected with replication-incompetent mutants. *J Virol* **64:** 4288–4295.

Krause PR, Croen KD, Straus SE, Ostrove JM (1988). Detection and preliminary characterization of herpes simplex virus type 1 transcripts in latently infected human trigeminal ganglia. *J Virol* **62:** 4819–4823.

Leib DA, Bogard CL, Kosz-Vnenchak M (1989). A deletion mutant of the latency-associated transcript of herpes simplex virus type 1 reactivates from the latent state with reduced frequency. *J Virol* **63:** 2893–2900.

Mehta A, Maggioncalda J, Bagasra O, Thikkavarapu S, Saikumari P, Valyi-Nagy T, Fraser NW, Block, TM (1995). *In situ* DNA PCR and RNA hybridization detection of herpes simplex virus sequences in trigeminal ganglia of latently infected mice. *Virology* **206:** 633–640.

Ramakrishnan R, Levine M, Fink DJ (1994). PCR-based analysis of herpes simplex virus type 1 latency in the rat trigeminal ganglion established with a ribonucleotide reductase-deficient mutant. *J Virol* **68**(11): 7083–7091.

Ramakrishnan R, Poliani PL, Levine M, Glorioso JC, Fink DJ (1996). Detection of herpes simplex virus type 1 latency-associated transcript expression in trigeminal ganglia by *in situ* reverse transcriptase PCR. *J Virol* **70**(9): 6519–6523.

Rock DL, Nesbern AB, Ghiasi H, Ong J, Lewis TL, Lokensgard JR, Wechsler S (1987). Detection of latency-related viral RNAs in trigeminal ganglia of rabbits latently infected with herpes simplex virus type 1. *J Virol* **61:** 3820–3826.

Rodahl E, Stevens JG (1992). Differential accumulation of herpes simplex virus type 1 latency-associated transcripts in sensory and autonomic ganglia. *Virology* **189:** 385–388.

Roizman B, Sears A (1996). Herpes simplex viruses and their replication. In: *Fields Virology*. Fields BN, Knipe DM, Howley PM, Chanock RM, Hirsch MS, Melnick JL, Monath TP, Roizman B (eds). 3rd. ed., vol. 2, Philadelphia: Lippincott-Raven, pp 2231–2295.

Sawtell NM (1997). Comprehensive quantification of herpes simplex virus latency at the single-cell level. *J Virol* **71**(7): 5423–5431.

Sawtell NM (1998). The probability of *in vivo* reactivation of herpes simplex virus type 1 increases with the number of latently infected neurons in the ganglia. *J Virol* **72**(8): 6888–6892.

Sawtell NM, Poon DK, Tansky CS, Thompson RL (1998). The latent herpes simplex virus type 1 genome copy number in individual neurons is virus strain specific and correlates with reactivation. *J Virol* **72**(7): 5343–5350.

Sedarati F, Izumi KM, Wagner EK, Stevens JG (1989). Herpes simplex virus type 1 latency-associated transcription plays no role in establishment or maintenance of a latent infection in murine sensory neurons. *J Virol* **63:** 4455–4458.

Steiner I, Spivack JG, O'Boyle DR, Lavi E, Fraser NW (1988). Latent herpes simplex virus type 1 transcription in human trigeminal ganglia. *J Virol* **62**(9): 3493–3496.

Stevens JG, Haarr L, Porter DD, Cook ML, Wagner EK (1988). Prominence of the herpes simplex virus latency-associated transcript in trigeminal ganglia from seropositive humans. *J Infect Dis* **158**(1): 117–123.

Stevens JG, Wagner EK, Devi-Rao GB, Cook ML, Feldman LT (1987). RNA complementary to a herpesvirus a gene mRNA is prominent in latently infected neurons. *Science* **235:** 1056–1059.

Thompson RL, Sawtell NM (1997). The herpes simplex virus type 1 latency-associated transcript gene regulates the establishment of latency. *J Virol* **71**(7): 5432–5440.

Trousdale MD, Steiner I, Spivack JG, Deshmane SL, Brown SM, MacLean AR, Subak-Sharpe JH, Fraser NW (1991). *In vivo* and in vitro reactivation impairment of a herpes simplex virus type 1 latency-associated trancript variant in a rabbit eye model. *J Virol* **65**: 6989–6993.